DALTON
FULL PAPER

Synthesis, characterisation, and molecular and electronic structure of $CpMoCl_2(R^1C{\equiv}CR^2)$ (R^1, R^2 = Ph, Et, Me): a new class of half-sandwich 17-electron molybdenum(III) organometallics

Erwan Le Grognec, Rinaldo Poli * and Philippe Richard

Laboratoire de Synthèse et d'Electrosynthèse Organometallique, Faculté des Sciences "Gabriel", Université de Bourgogne, 6 Boulevard Gabriel, 21100 Dijon, France.
E-mail: Rinaldo.Poli@u-bourgogne.fr

Received 3rd February 2000, Accepted 9th March 2000
Published on the Web 3rd April 2000

Addition of alkyne to $[CpMoCl_2]_2$ affords compounds $CpMoCl_2(\eta^2$-alkyne) (alkyne = EtC≡CMe, **1**; EtC≡CEt, **2**; PhC≡CMe, **3**; PhC≡CPh, **4**) in good yields. The compounds have been characterised by C,H analyses, IR, EPR and mass spectroscopies, magnetic susceptibility, and cyclic voltammetry. In addition, a single crystal X-ray diffraction analysis has been carried out for compound **4.** The alkyne ligand adopts an almost parallel conformation relative to the Cp ring, essentially identical with that of previously reported Nb, Ta, and W analogues. Geometry optimisations on the $CpMCl_2(HC{\equiv}CH)$ (M = Nb, Mo) model compounds show that the total energy is nearly independent of the alkyne orientation. The SOMO for M = Mo is an essentially metal-based orbital with a slight Mo-Cl π* component, in agreement with the observed trends in M–Cl bond lengths on going from Group 5 to Group 6. The cyclic voltammetric behaviour of **1**–**4** is similar to the analogous diene complexes $CpMoCl_2(\eta^4$-diene). A reaction between **1**–**4** and excess alkyne takes place only for the dialkylsubstituted alkyne complexes under forcing conditions. Compound $CpMoCl_2(\eta^4$-$C_4Et_4H)$, **5**, has been isolated from the reaction between **2** and excess EtC≡CEt and crystallographically characterized.

Introduction

Alkyne organometallic chemistry has always attracted much attention because of the versatility of alkynes in metal-mediated organic synthesis and catalysis[1–5] and more recently also for their application in materials chemistry.[6–9] Group 6 alkyne chemistry is quite extensively studied, the vast majority of the investigations concerning compounds where the metal has the formal oxidation state II.[10–12] The interactions of alkynes with Group 6 metals in the oxidation state III are mostly related to dinuclear M_2X_6-type (M = Mo, W)[1,3,13] and $[(C_5H_4R)WCl_2]_2$ (R = Me, Pr^i)[14–18] compounds. A few mononuclear M(III)-alkyne complexes, however, have been described both for Mo and for W, *e.g.* $WCl_3(PMe_3)_2$(PhC≡CPh),[19] [Tp*WX(CO)(MeC≡CMe)][BF_4] [Tp* = hydrotris(3,5-dimethylpyrazolyl)borate; X = F, Cl, Br or I],[20] [$MoCl_3(THT)_2$(PhC≡CR)] (R = Me, Et, THT = tetrahydrothiophene),[21] and $Mo(NPr^iAr)_3$(PhC≡CPh) (Ar = 3,5-$C_6H_3Me_2$).[22]

Paramagnetic half-sandwich compounds of general formula $(\eta^5$-$C_5R_5)MCl_2$(alkyne) (M = Group 6 metal) appear limited to two related examples for tungsten. The reaction between $W(\equiv CBu^t)Cl_3$(dme) and excess RC≡CR yields $(\eta^5$-$C_5R_4Bu^t)$-WCl_2(RC≡CR) (R = Me, Et),[23] the structure of the 2-butyne adduct being confirmed by an X-ray analysis.[24] These reactions are not selective and do not appear of potentially general synthetic utility. In addition, the reduction of Cp^*WX_4 (X = OPh, Cl) with sodium amalgam in the presence of alkynes was reported to afford the corresponding W(II) species Cp*WX-(alkyne)$_2$ with no mention of W(III) intermediates.[25]

For molybdenum, it has been shown that the treatment of $CpMoCl(CF_3C{\equiv}CCF_3)_2$ with dienes involves a disproportionation process resulting in the isolation of the Mo(III)-diene products $CpMoCl_2$(diene).[26–28] Whether this transformation involves Mo(III)-alkyne or Mo(II)-diene intermediates does not appear to have been the subject of investigations. We have more recently prepared the same diene compounds by the high-yield, straightforward addition of diene to $[CpMoCl_2]_2$.[29,30] It has also been reported that the thermal treatment of CpMoCl(PhC≡CPh)$_2$ affords several rearrangement products, including the 17-electron Mo(III) cyclobutadiene complex $CpMoCl_2(\eta^4$-$C_4Ph_4)$.[31,32] No mention was made, however, whether an alkyne complex of formula $CpMoCl_2(\eta^2$-$C_2Ph_2)$ also forms. Since the direct addition of neutral ligands to $[CpMoCl_2]_2$ appears to be a versatile method to obtain half-sandwich Mo(III) derivatives under mild conditions,[33] we have explored this methodology for the preparation of alkyne adducts and report here the successful synthesis and studies of four members of the hitherto unreported $CpMoCl_2$(alkyne) family.

Results and discussion

The addition of alkynes $R^1C{\equiv}CR^2$ to a THF suspension of $[CpMoCl_2]_2$ at the THF reflux temperature yields the soluble adducts $CpMoCl_2(R^1C{\equiv}CR^2)$ according to eqn. (1). Thermal

$$[CpMoCl_2]_2 + 2\ R^1C{\equiv}CR^2 \longrightarrow 2\ CpMoCl_2(R^1C{\equiv}CR^2) \quad (1)$$

(**1**: R^1=Me, R^2=Et; **2**: R^1=R^2=Et; **3**: R^1=Me, R^2=Ph; **4**: R^1=R^2=Ph)

decomposition of the products does not take place under these conditions and all products were recovered in good to excellent yields. The rate of the reaction decreases in the order **1**,**2** > **3** > **4**, compound **1** being also obtained within a reasonable time (4 h) when the reaction is conducted at room temperature. For compound **4**, an excess of alkyne may be used with no detriment to the yield, and no reaction occurs upon prolonged treatment of isolated **4** with a second equivalent of diphenylacetylene in refluxing THF. For compounds **1** and **2**, on the other hand, the stoichiometric amount of alkyne must be used in order to avoid the formation of by-products (*vide infra*).

It is interesting to observe that while the alkyne addition to the corresponding tungsten starting materials, $[(C_5H_4R)WCl_2]_2$

This journal is © The Royal Society of Chemistry 2000

(R = Me or Pr^i), gave only the dinuclear, metal–metal bonded products $(C_5H_4R)_2W_2Cl_4(\mu\text{-}C_2R'_2)$ or $(C_5H_4R)_2W_2Cl_4(\mu\text{-}C_4R'_4)$ depending on stoichiometry and conditions,[14–16] reaction (1) produces only mononuclear paramagnetic products, in agreement with the reduced strength of the Mo–Mo bond relative to the W–W bond in the starting material. The mononuclear (η^5-$C_5R_4Bu^t$)WCl_2(RC≡CR) (R = Me, Et) complexes,[23] analogous to our compounds **1**–**4**, were obtained by a different synthetic strategy starting from a mononuclear carbyne precursor. It is also of relevance that the reaction between $[(C_5H_4Pr^i)MoCl_2]_2$ and 2-butyne was mentioned to afford intractable products.[34]

Compounds **1**–**4** are air sensitive but can be stored in the solid state under argon without significant decomposition. They are readily soluble in THF and CH_2Cl_2, only partially soluble in diethyl ether and completely insoluble in pentane. Satisfactory C, H elemental analyses for **3** and **4** could only be obtained in the presence of V_2O_5 as a combustion catalyst. The IR spectra confirm the presence of coordinated alkyne ligands, a weak ν(C≡C) absorption being observed at 1730 cm^{-1} for **1**, 1732 for **2**, 1717 cm^{-1} for **3** and 1700 cm^{-1} for **4**, *i.e.* >400 cm^{-1} lower relative to the free alkynes. Although the quantitative relationship between stretching frequency and C–C bond order does not appear to have been carefully explored, larger shifts are usually associated with the 4-electron ($\sigma + \pi$) coordination mode, the largest observed shifts being around 450 cm^{-1}.[2] The mass spectra show the molecular ion for each compound, in agreement with a mononuclear formulation. The mononuclear nature of the products is also consistent with the paramagnetism, as indicated by the EPR spectra in solution at room temperature and confirmed by the magnetic susceptibility measurement for **1**, **3** and **4**, yielding a magnetic moment close to the spin-only value for one unpaired electron.

The EPR spectra are characterised by a sharp isotropic signal at room temperature, while frozen solutions at low temperatures show an essentially tetragonal ***g*** tensor. This is as expected for the 17-electron configuration of the complexes (when considering the alkyne as a $\sigma + \pi$ 4-electron donor). In this respect, compounds **1**–**4** are perfectly isoelectronic with the growing class of $CpMoX_2L_2$ compounds.[35] Molybdenum satellites due to ^{95}Mo(15.9%) and ^{97}Mo(9.5%), both having $I = 5/2$, are visible for both the isotropic spectrum and the perpendicular component of the frozen solution spectrum (see Table 1). A nearly tetragonal ***g*** tensor was also observed for the related alkyne complexes of W(III), [Tp*WX(CO)(MeC≡CMe)][BF_4] (X = F, Cl, Br, I).[20]

A mononuclear formulation is finally confirmed by the X-ray structure of **4**, which is illustrated in Fig. 1. The most relevant feature of the geometry is the three-legged piano stool disposition, with the alkyne ligand adopting a conformation almost parallel to the Cp plane. The angle θ between the Mo–C(6)–C(7) plane and the plane defined by Mo, CNT (center of gravity of the Cp ring), and the midpoint of the C(6)–C(7) vector is 85.61°. This tilting away from the ideal parallel conformation ($\theta = 90°$) is less pronounced relative to the previously reported W(III) complex (η^5-$C_5Me_4Bu^t$)WCl_2(MeC≡CMe) (θ = 77.16°)[24] and slightly more relative to Cp*$TaCl_2$(PhC≡CPh) ($\theta = 87.27°$)[36] and (η^5-C_5H_4Me)$NbCl_2$(ArC≡CAr) (Ar = $C_6H_4CH_3$-4, $\theta = 86.40°$).[37]

Table 2 collects relevant bond distances and angles, in comparison with those of the above mentioned Nb analogue (η^5-C_5H_4Me)$NbCl_2$(ArC≡CAr)[38] and of geometry optimised HC≡CH model compounds (*vide infra*). It can be seen from Table 2 that while the M–CNT and M–C(alkyne) distances are significantly shorter for Mo relative to Nb, the M–Cl distances are

Table 1 EPR parameters for compounds **1**–**4** in CH_2Cl_2 : THF (1 : 2)

	T = 298 K		T = 100 K		
	g_{iso}	$\lvert A_{iso}\rvert$	$g_\parallel$	$g_\perp$	$\lvert A_\perp^{Mo}\rvert$
1	1.987	37.5	2.043	1.970	63.0
2	1.987	37.5	2.043	1.969	63.2
3	1.988	38.6	2.040	1.971	61.5
4	1.989	38.9	2.038	1.971	61.7

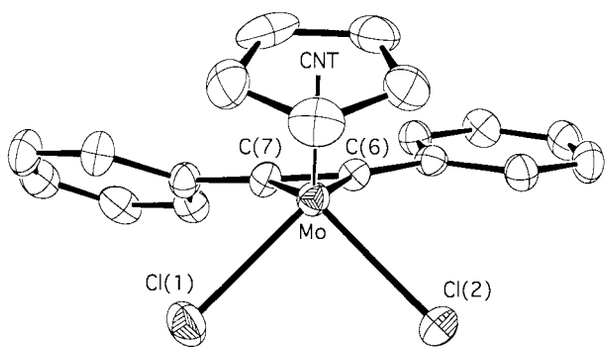

Fig. 1 An ORTEP[57] view of compound **4** with thermal ellipsoids drawn at the 30% probability level. Hydrogen atoms are omitted for clarity.

Table 2 Comparison between experimental and calculated bond distances and angles for compounds $CpMCl_2$(alkyne) (M = Nb, Mo)

	M = Nb		M = Mo	
	Experimental[a]	Optimised[b]	Experimental[c]	Optimised[b]
M–CNT	2.113	2.180	2.010(5)	2.087
M–Cl	2.365(2)	2.426	2.375(9)	2.423
M–Cl	2.353(2)	2.426	2.370(9)	2.423
M–C	2.079(5)	2.096	2.034(3)	2.056
M–C	2.063(5)	2.096	2.021(3)	2.056
C≡C	1.307(7)	1.328	1.303(4)	1.324
CNT–M–Cl	115.7	114.38	120.6(3)	117.29
CNT–M–Cl	115.2	114.38	116.0(4)	117.29
CNT–M–C	111.9	114.88	113.3(3)	116.09
CNT–M–C	114.1	114.88	116.0(4)	116.09
Cl–M–Cl	99.4(1)	101.69	89.12(4)	91.93
C–M–C	36.8(2)	36.93	37.47(11)	37.56
M–C≡C	72.3(3)	71.54	71.8(2)	71.22
M–C≡C	70.9(3)	71.54	70.7(2)	71.22
C–C≡C	142.3	145.97	145.1(3)	143.53
C–C≡C	144.3	145.97	145.8(3)	143.53

[a] For compound (η^5-C_5H_4Me)$NbCl_2$(ArC≡CAr) (Ar = $C_6H_4CH_3$-4) (ref. 37); the figures without standard deviations were calculated from the published crystal data. [b] For the model compounds $CpMCl_2$(HC≡CH) with a parallel orientation of the ethyne ligand. [c] For compound **4**.

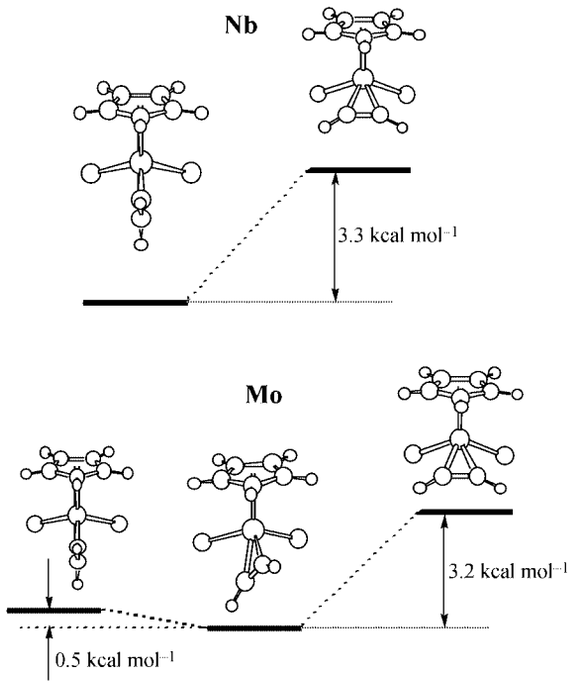

Fig. 2 B3LYP/LANL2DZ total energies for $CpMCl_2(HC{\equiv}CH)$ (M = Nb, Mo) at different ethyne conformations.

essentially identical. The same trend can be noticed by comparing the previously described $Cp^*TaCl_2(PhC{\equiv}CPh)$ and $(\eta^5\text{-}C_5Me_4Bu^t)WCl_2(MeC{\equiv}CMe)$.[24,36] A general shortening is expected as a result of the smaller atomic radius of a Group 6 metal relative to the corresponding Group 5 metal in the same row and formal oxidation state. The alkyne C–C distance is essentially identical with that of the Nb complex (Table 2) and of the W complex (1.312(10) Å),[24] while this is longer in the Ta compound (1.337(8) Å).[36] In other structurally characterised Mo(III)-alkyne complexes, *e.g.* $MoCl_3(THT)_2(PhC{\equiv}CR)$ (THT = tetrahydrothiophene; R = Me, Et),[21] the alkyne C–C distance is less accurately determined but does not appear to be significantly different than for compound **4** (*i.e.* 1.27(1), 1.31(1) and 1.32(1) Å). The C–C≡C–C framework is quite bent (C–C≡C angles around 145°), only slightly less so than in the above mentioned Ta, W and Nb compounds (averages of 139.4(9), 140.3(7)° and 143.3(10)°, respectively). Together with the C≡C distance, this parameter confirms that the alkyne ligand acts as a four-electron donor.

The bonding features of this class of alkyne complexes has been further investigated at the theoretical level. The electronic structure for $CpMCl_2$(alkyne) systems has only been previously explored by Curtis *et al.* for M = Nb at the extended Huckel level, at the fixed geometry determined by X-ray diffraction.[37] We have carried out geometry optimisations at the B3LYP/LANL2DZ level on the model compound $CpMoCl_2(HC{\equiv}CH)$. As is now well established, this level of theory affords satisfactory geometries and energies for medium-size organometallic compounds. A full optimisation indeed yields a geometry with bond distances and bond angles close to the experimental values. As is typical for this computational technique, distances are slightly overestimated (up to 0.07 Å), whereas bond angles are reproduced to within 3°. However, the orientation of the ethyne ligand is quite different from experiment, θ being only 30.78°.

Subsequent optimisations have been carried out with the ethyne ligand forced to adopt a parallel and a perpendicular orientation by imposing a C_s symmetry to the molecule. The results (Fig. 2) show that the total energy is almost independent on the alkyne orientation and suggest that the adoption of a close to parallel geometry for compound **4** [and by extension also by the tungsten analogue $(\eta^5\text{-}C_5Me_4Bu^t)WCl_2(MeC{\equiv}CMe)$] is due to the minimisation of the steric repulsion between the cyclopentadienyl and alkyne ligands. The optimised parameters reported in Table 2 are those of the parallel geometry, which is closest to the experimentally determined geometry.

Analogous calculations have been carried out on the niobium model system $CpNbCl_2(HC{\equiv}CH)$, the results being also shown in Fig. 2. In this case, a full optimisation leads to an essentially C_s-symmetric geometry with a perpendicular ethyne ligand. The C_s-imposed parallel orientation is found, like for Mo, to have an energy very close to that of the perpendicular conformation. The optimised distances and angles reported in Table 2 are those relating to the parallel geometry, which is closest to the experimental structure. A comparison between calculated and experimental parameters shows again the adequacy of the computational method. It seems, therefore, that the choice of geometry for Group 5 $CpMCl_2$(alkyne) compounds, like for the analogous Group 6 compounds, is dictated by the steric requirements.

Additional insights are given by the orbital analysis. The energy and shape of relevant Kohn–Sham orbitals retrieved from the DFT calculations are shown in Fig. 3 for both Nb and Mo systems with the ethyne ligand both in the perpendicular and in the parallel conformation. For the Mo complex, only the α spin orbitals are shown (the shapes of the corresponding β spin orbitals are essentially identical), while the energy reported is the average of α and β. Orbital no. 38 is the HOMO for the Nb system while the Mo system has an additional unpaired electron in orbital no. 39. The latter is essentially a metal-based orbital. However, there is a significant participation of Cl lone pairs for the Mo system, giving rise to a Mo–Cl π* combination. This rationalises why, on going from Nb to Mo, the M–Cl bond length does not significantly shorten: the effect of the metal radius reduction is compensated by the Mo–Cl π* contribution of the additional electron. The alkyne-to-M π interaction ($\pi_\perp$) gives a bonding combination which is evident in orbital no. 28, and the corresponding antibonding component in orbital no. 40. The alkyne-to-M σ donation is in a deeper energy orbital, while the orbitals no. 29–37 (not shown) contain the M–Cl σ bonds, the Cl p lone pairs, and the M–Cp σ and π interactions. There is heavy symmetry-allowed mixing of various bonding components in individual orbitals. Orbital no. 38 contains the M–alkyne π back-bonding interaction ($\pi_\parallel$). Its lower energy and greater percentage contribution of metal and alkyne orbitals for M = Nb suggests a greater degree of back-bonding for this metal, in agreement with the observed structural differences (*vide supra*).

Fig. 3 allows one to appreciate the reason for the small dependence of the total energy on the alkyne configuration. The alkyne ligand is able to establish both π interactions with the metal center no matter what the relative orientation of alkyne and M–Cp axis. In a reference system where z coincides with the M–CNT vector and the alkyne midpoint lies on the xz plane, the perpendicular conformation involves a $\pi_\perp$ interaction with an essentially xy metal orbital and a $\pi_\parallel$ interaction with a $(x^2 - z^2)$ orbital, whereas the same two metal orbitals trade places on going to the parallel conformation. Thus, these two orbitals may generate linear combinations suitable to establish equally efficient $\pi_\perp$ and $\pi_\parallel$ interactions for any alkyne conformation, effectively following the rotation of the alkyne ligand around the Mo–alkyne axis. For this reason, little or no electronic barrier is expected against alkyne rotation and the observed conformation is largely determined, for both Group 5 and 6 metals, by the intramolecular steric interactions.

The electrochemical investigation of compounds **1**–**4** by cyclic voltammetry reveals both a one-electron reduction and a one-electron oxidation process. The reduction wave appears at relatively large negative potentials *vs.* the ferrocene standard (see Table 3) and is reversible ($i_a/i_c = 1$, ΔE_p *ca.* 60 mV) for compounds **3** and **4** in the 100–5000 mV s^{-1} range of scan speeds. For compounds **1** and **2**, on the other hand, the reduction wave

becomes reversible only above 2000 mV s^{-1} and, at lower scan speeds, the i_a/i_c becomes smaller and smaller. Since no new wave appears in the voltammogram at low scan rate, the reduction products $[\mathbf{1}]^-$ and $[\mathbf{2}]^-$ must decompose to redox-inactive species which remain so far uncharacterised. The oxidation process, on the other hand, is completely irreversible up to 5 V s^{-1} for all derivatives. In this respect, these compounds behave similarly to the previously described diene complexes, $CpMoCl_2(\eta^4\text{-diene})$,[26–28,30] while derivatives with more electron donating ligands (phosphines, phosphine-thioethers, phosphine-oxazolines, and phosphine-amides)[35,39,40] show a reversible oxidation process at much lower potentials and no reduction process or, at the most, an irreversible reduction before the solvent discharge. A closer comparison of the reduction potentials between the isoelectronic complexes with the 4-electron donors alkyne ($\sigma + \pi$) and diene (2σ) ligands in Table 3 indicates that the alkynes transfer about the same amount of electron density to the metal center. The negative shift of the reduction potential on going from the less alkyl substituted alkyne complex **4** to the more alkyl substituted complexes **1** and **2** is in agreement with the greater electron-donating properties of alkyls. The same trend is observed for the oxidation potentials (**1**,**2** < **3** < **4**). However, the potentials of the oxidation processes will also reflect the kinetics of the follow-up chemical processes and cannot be used as a thermodynamic gauge of the metal electron density.

Table 3 Cyclic voltammetric data for compounds **1**–**4** in THF at room temperature and comparison with related η^4-diene complexes

Compound	$E_{1/2}(Mo^{II}/Mo^{III})$	$E_{p.a}(Mo^{III}/Mo^{IV})$[a]	Ref.
$CpMoCl_2(\eta^2\text{-EtC}\equiv\text{CMe})$, **1**	−1.32	0.14	This work
$CpMoCl_2(\eta^2\text{-EtC}\equiv\text{CEt})$, **2**	−1.33	0.16	This work
$CpMoCl_2(\eta^2\text{-PhC}\equiv\text{CMe})$, **3**	−1.20	0.22	This work
$CpMoCl_2(\eta^2\text{-PhC}\equiv\text{CPh})$, **4**	−1.14	0.32	This work
$CpMoCl_2(\eta^4\text{-}C_4H_6)$	−1.11	0.73	28,56
$CpMoCl_2(\eta^4\text{-}C_4H_5Me\text{-}2)$	−1.19	0.75	56
$CpMoCl_2(\eta^4\text{-}C_4H_4Me_2\text{-}2,3)$	−1.24	0.66	56

[a] All potentials are measured at a scan rate of 200 mV s^{-1}.

When reaction (1) was carried out in the presence of excess diphenylacetylene, no detriment to the yields of **4** and no additional product were observed. However, a second resonance grows in the EPR spectrum for the 2-pentyne and 3-hexyne reactions with an excess of the alkyne under forcing conditions. The 3-hexyne reaction has been subjected to more detailed investigations. A new compound (characterised by an EPR resonance at $g = 1.996$; $a_{Mo} = 34.6$ G) forms only quite slowly and a complete consumption of **2** was achieved only upon prolonged reflux in neat 3-hexyne (bp 82 °C). The reaction, however, is not selective and the Mo-containing, EPR active product could not be obtained in a pure form. However, a mass spectrum of the crude product mixture exhibits, in addition to the peaks of **2**, peaks attributable to a compound of formula $CpMoCl_2(C_4Et_4)$. On the basis of the existence of the cyclobutadiene complex $CpMoCl_2(\eta^4\text{-}C_4Ph_4)$[31,32] and on the EPR properties which indicate a 17-electron species, we tentatively suggest a cyclobutadiene structure also for this compound. Crystallization of the crude product from this reaction afforded instead a small amount of the previously reported[41] $CpMoCl_2(\eta^4\text{-}C_4Et_4H)$, **5**.

The NMR properties for the isolated crystals of **5** match with those previously reported[41] and a single crystal X-ray analysis (see Fig. 4 and Table 4) confirms the structural assignment. In particular, the hydrogen atom of the η^4(5e)-butadienyl ligand was directly located from the difference Fourier map and freely refined. While the quality of the data affords metric parameters of greater precision, the structural parameters of **5** compare quite closely with those previously reported for the analogous $CpMoBr_2(\eta^4\text{-}C_4Et_4H)$.[41] No further discussion of the structure of **5** is therefore warranted here, except for pointing out that the structural data and the NMR data concur in interpreting the metal–butadienyl bonding mode as mostly **I** (Fig. 5).

We presume that, under the forcing conditions used for the reaction with excess alkyne, a hydrogen atom abstraction from the medium by either the cyclobutadiene product or by a reaction intermediate may be responsible for the formation of **5**. This compound was previously obtained starting from a bis-alkyne Mo(II) precursor, where the C–C coupling process was presumed to follow the protonation of one alkyne ligand to

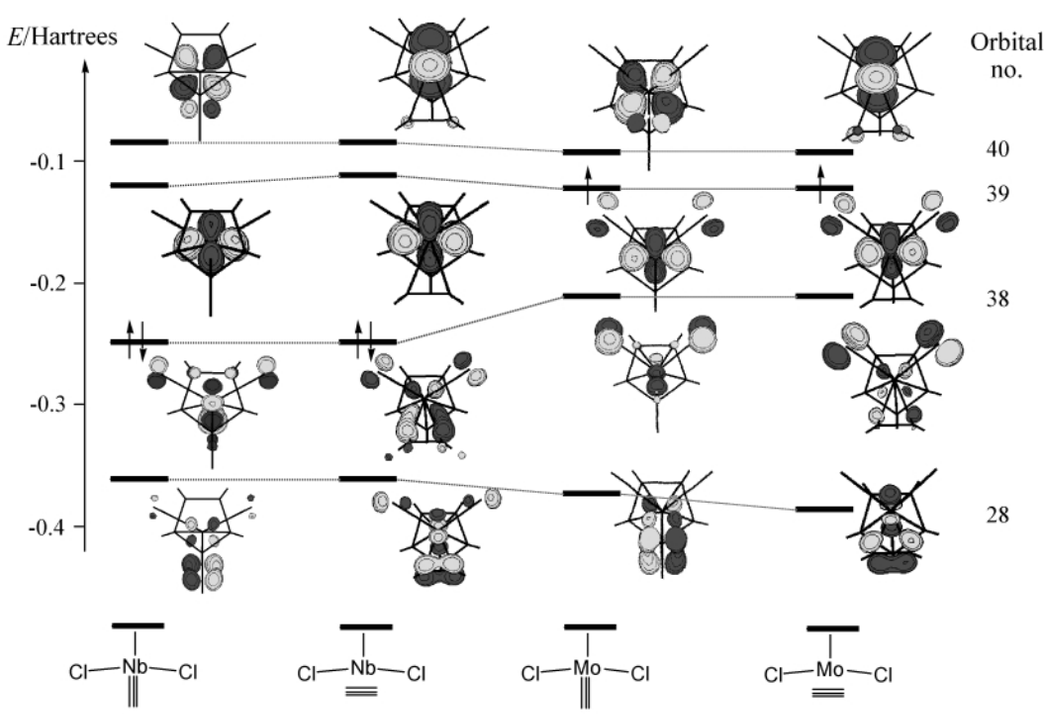

Fig. 3 Energy and shape of relevant orbitals for $CpMCl_2(HC\equiv CH)$ (M = Nb, Mo).

Table 4 Selected bond distances (Å) and angles (°) for compound **5**

Mo–CNT	1.986(3)	Mo–C(8)	2.444(2)
Mo–Cl(1)	2.4652(7)	Mo–C(9)	2.303(3)
Mo–Cl(2)	2.4874(6)	C(6)–C(7)	1.438(4)
Mo–C(6)	1.934(2)	C(7)–C(8)	1.404(4)
Mo–C(7)	2.329(2)	C(8)–C(9)	1.440(4)
CNT–Mo–Cl(1)	112.6(2)	C(9)–Mo–Cl(1)	137.51(7)
CNT–Mo–Cl(2)	111.7(2)	C(7)–Mo–Cl(1)	84.55(7)
CNT–Mo–C(6)	106.5(2)	C(6)–Mo–Cl(2)	140.61(8)
CNT–Mo–C(9)	109.7(2)	C(9)–Mo–Cl(2)	80.85(7)
Cl(1)–Mo–Cl(2)	80.36(2)	C(7)–C(6)–Mo	86.0(2)
C(6)–Mo–C(9)	77.52(10)	C(8)–C(9)–Mo	77.8(2)
C(6)–Mo–C(7)	38.02(10)	C(10)–C(6)–Mo	147.9(2)
C(9)–Mo–C(7)	63.06(9)	C(16)–C(9)–Mo	126.2(2)
C(3)–Mo–C(7)	131.65(9)	C(8)–C(9)–C(16)	122.9(2)
C(6)–Mo–C(8)	65.26(9)	C(7)–C(6)–C(10)	126.1(2)
C(9)–Mo–C(8)	35.16(9)	C(8)–C(7)–C(6)	115.2(2)
C(7)–Mo–C(8)	34.11(9)	C(7)–C(8)–C(9)	116.8(2)
C(6)–Mo–Cl(1)	93.97(8)		

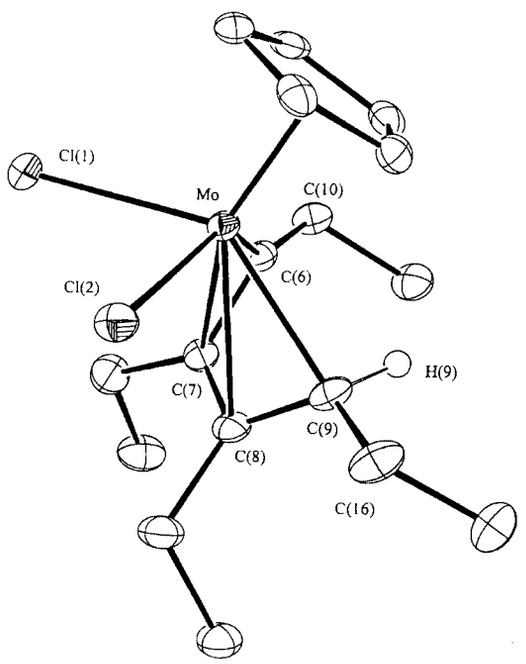

Fig. 4 An ORTEP view of compound **5** with thermal ellipsoids drawn at the 50% probability level. Hydrogen atoms except for H(9) of the η^4(5e)-butadienyl ligand are omitted for clarity.

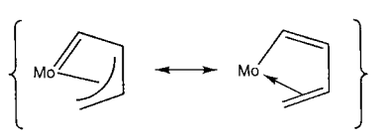

Fig. 5 Possible bonding modes for the butadienyl ligand.

afford a reactive alkyne–vinyl intermediate.[41] A similar process has also been observed for related dithiocarbamato derivatives of Mo(II) and W(II).[42]

The failure to obtain the previously reported tetraphenylcyclobutadiene complex from **4** + PhC≡CPh means that the barrier to the 2 + 2 cycloaddition reaction must be prohibitively high, higher than for the **2** + EtC≡CEt reaction, on this metal system. Thus, the reported formation of $CpMoCl_2$-(η^4-C_4Ph_4) by thermolysis of CpMoCl(PhC≡CPh)$_2$ [31,32] most likely does not involve compound **4** as an intermediate, while a more likely possibility is oxidative coupling of the alkyne ligands to generate a CpMoCl(η^4-C_4Ph_4) intermediate which subsequently disproportionates. It is notable that alkyne dimerization occurs on a mononuclear CpMo(III) species, whereas for related tungsten chemistry the same process occurs on a dinuclear CpW(III) species.[14–16]

Conclusions

The alkyne addition to $[CpMoCl_2]_2$ provides a facile entry to hitherto unknown half-sandwich Mo(III) alkyne complexes under mild conditions. The electronic structure of these complexes is quite similar to that of the corresponding Group 5 derivatives, the additional electron residing in an essentially pure metal orbital which is not engaged in the metal–alkyne interaction. As a consequence, the nature of the metal–alkyne interaction is rather similar for Group 5 and Group 6 compounds, including the slight dependence of the energy on the alkyne conformation. On the other hand, the oxidation to afford isoelectronic species with the Group 5 complexes is irreversible, while the reduction to anionic 18-electron complexes is reversible on the cyclic voltammetric time scale. The electrochemical investigations further indicate that the $CpMoCl_2$(η^2-alkyne) system is about as electron-rich as the $CpMoCl_2$(η^4-diene) system, while the reactivity study shows that a 2 + 2 cycloaddition to afford a cyclobutadiene system has a high activation barrier for this system.

Experimental

All reactions involving air- and moisture-sensitive organometallic compounds were carried out in a Jacomex glove box or by the use of standard Schlenk techniques under an argon atmosphere. The solvents were dried by conventional methods (THF, Et_2O, toluene and pentane from sodium benzophenone ketyl and CH_2Cl_2 from P_4O_{10}) and distilled under argon prior to use. EPR measurements were carried out at the X-band microwave frequency on a Bruker ESP300 spectrometer. All EPR spectral parameters for the new compounds are collected in Table 1. The spectrometer frequency was calibrated with DPPH (diphenylpicrylhydrazyl, $g = 2.0037$). Cyclic voltamograms were recorded with an EG&G 362 potentiostat connected to a Macintosh computer through MacLab hardware/software. The electrochemical cell was fitted with a Ag/AgCl reference electrode, a platinum disk working electrode and a Pt wire counterelectrode. Bu_4NPF_6 (*ca.* 0.1 M) was used as supporting electrolyte. All potentials are reported relative to the ferrocene standard, which was added to each solution and measured at the end of the experiments. All the voltammetric results obtained in this study are collected in Table 3. The mass spectra were obtained by electron impact at 70 eV on a Kratos Concept 32S spectrometer by direct introduction of solid samples. The magnetic susceptibility measurements were carried out at room temperature with a Johnson Matthey magnetic balance which operates with a modified Gouy method, whereby the effect of the sample on the weight of the magnet, rather than the effect of the magnet on the weight of the sample, is used to retrieve the susceptibility information. The elemental analyses were carried out by the analytical service of the Laboratoire de Synthèse et d'Electrosynthèse Organométallique with a Fisons EA 1108 apparatus. EtC≡CMe, EtC≡CEt, PhC≡CMe, PhC≡CPh were purchased from Aldrich Chemical Co. and used as received. Compound $[CpMoCl_2]_2$ was prepared as described in the literature.[43,44]

Synthesis of $CpMoCl_2$(η^2-EtC≡CMe), 1

To a suspension of $[CpMoCl_2]_2$ (0.668 g, 1.44 mmol) in 20 mL of THF was added 2-pentyne (277 μL, 2.88 mmol) *via* a syringe. The mixture was then refluxed for 30 minutes, transforming the initial pale brown suspension to a dark brown solution. This solution was filtered through Celite and evaporated to dryness to yield an oily residue. Diethyl ether (10 mL) was added and the suspension was vigorously stirred to afford **1** as a brown

powder. The supernatant was decanted off and the solid was washed with several portions of pentane (total *ca.* 30 mL). Yield: 0.604 g, 70%. Anal. Calc. for $C_{10}H_{13}Cl_2Mo$: C, 40.03; H, 4.37. Found: C, 40.32; H, 4.22%. IR (Nujol mull, cm^{-1}): 1730 [m, ν(C≡C)], MS (EI, 70 eV): *m*/*z* 301, $[M]^+$ ($MoCl_2$ pattern, 2%); 233 $[CpMoCl_2]^+$ ($MoCl_2$ pattern, 6%), 68 $[EtC{\equiv}CMe]^+$ (47%). $\mu_{eff} = 1.60\mu_B$ (diamagnetic correction = -148×10^{-6} cgsu).

Synthesis of $CpMoCl_2(\eta^2$-EtC≡CEt), 2

To a suspension of $[CpMoCl_2]_2$ (0.905 g, 1.95 mmol) in 20 mL of THF was added 3-hexyne (440 μL, 3.9 mmol) *via* a syringe. The mixture was then refluxed for 2 h, transforming the initial pale brown suspension to a dark brown solution. This solution was filtered through Celite and evaporated to dryness to yield an oily residue. The product **2** was extracted with 40 mL of refluxing diethyl ether. Following filtration of the hot solution, crystals formed upon cooling to 4 °C. The supernatant was decanted off and the crystals were dried *in vacuo*. Yield: 0.612 g, 50%. Anal. Calc. for $C_{11}H_{15}Cl_2Mo$: C, 42.07; H, 4.80. Found : C, 41.63; H, 4.75%. IR (Nujol mull, cm^{-1}): 1732 [m, ν(C≡C)], MS (EI, 70 eV): *m*/*z* 315, $[M]^+$ ($MoCl_2$ pattern, 13%); 233 $[CpMoCl_2]^+$ ($MoCl_2$ pattern, 67%), 82 $[EtC{\equiv}CEt]^+$ (56%).

Synthesis of $CpMoCl_2(\eta^2$-PhC≡CMe), 3

To a suspension of $[CpMoCl_2]_2$ (0.720 g, 1.55 mmol) in THF in 20 mL was added 1-phenyl-1-propyne (388 μL, 3.1 mmol) *via* a syringe. The mixture was then refluxed for 2 hours yielding a red brown solution. The solution was filtered through Celite and concentrated to *ca.* 3 mL. Diethyl ether (10 mL) was then added under a vigorous stirring, precipitating a fine red-brown powder. The supernatant was cannulated off and the residue was washed with several portions of pentane (total *ca.* 50 mL). Yield: 0.750 g, 70%. Anal. (obtained in the presence of V_2O_5 as a combustion catalyst) Calc. for $C_{14}H_{13}Cl_2Mo$: C, 48.31; H, 3.76. Found: C, 48.16; H, 3.65%. IR (Nujol mull, cm^{-1}): 1717 [m, ν(C≡C)], MS (EI, 70 eV): *m*/*z* 349 $[M]^+$ ($MoCl_2$ pattern, 4%), 233 $[CpMoCl_2]^+$ ($MoCl_2$ pattern, 6%), 116 $[PhC{\equiv}CMe]^+$ (80%). $\mu_{eff} = 1.64\mu_B$ (diamagnetic correction = -157×10^{-6} cgsu).

Synthesis of $CpMoCl_2(\eta^2$-PhC≡CPh), 4

To a pale brown suspension of $[CpMoCl_2]_2$ (1.438 g, 3.1 mmol) in 40 mL of THF was added a THF solution of diphenylacetylene (1.3 g, 7.3 mmol). The mixture was heated to 70–80 °C for 2 hours, yielding a red solution. After cooling to room temperature, the solvent was reduced in volume to *ca.* 7 mL and pentane (30 mL) was added to complete the precipitation of the product. The supernatant was decanted off, and the brick-red powder was washed with several portions of pentane (total *ca.* 50 mL). Yield: 2.150 g, 85%. Recrystallisation by slow diffusion of pentane into a CH_2Cl_2 solution afforded dark red crystals. Anal. (obtained in the presence of V_2O_5 as a combustion catalyst) Calc. for $C_{19}H_{15}Cl_2Mo$: C, 55.64; H, 3.69. Found: C, 55.29; H, 3.65%. IR (Nujol mull, cm^{-1}): 1700 [m, ν(C≡C)], MS (EI, 70 eV): *m*/*z* 411 $[M]^+$ ($MoCl_2$ pattern, 2%), 233 $[CpMoCl_2]^+$ ($MoCl_2$ pattern, 6.5%), 178 $[PhC{\equiv}CPh]^+$ (100%). $\mu_{eff} = 1.61\mu_B$ (diamagnetic correction = -178×10^{-6} cgsu).

Reaction between 2 and excess EtC≡CEt

Compound **2** (50 mg, 0.16 mmol) was dissolved in 3-hexyne (2 mL) and the resulting red solution was refluxed for 15 h with EPR monitoring. The initial EPR signal ($g = 1.987$, $a_{Mo} = 37.5$) was slowly replaced by a new signal at $g = 1.996$, $a_{Mo} = 34.6$ G. During this time the color changed to dark yellow and a white precipitate formed. An aliquot of the final solution was evaporated to dryness and the residue was redissolved in the minimum amount of CH_2Cl_2 for the mass spectral analysis. MS (EI, 70 eV): *m*/*z* 397 $[M]^+$ ($MoCl_2$ pattern, 5%), 361 $\{[M]^+ - HCl\}$ (MoCl pattern, 3.8%). The remainder of the solution was evaporated to dryness and the residue was extracted with diethyl ether (5 mL) followed by filtration through Celite. The solution was concentrated to *ca.* half volume and a layer of pentane (5 mL) was left to diffuse slowly at room temperature. Red crystals of compound $CpMoCl_2(\eta^4$-$C_4Et_4H)$, **5**, formed within 1 week. One of the crystals was used for the X-ray analysis. ^{1}H NMR ($CDCl_3$): δ 5.32 (s, 5H, Cp), 3.28 (m, 2H, CH_2), 2.67 (m, 2H, CH_2), 2.58 (m, 2H, CH_2), 2.34 (m, 2H, CH_3CH_2CH), 2.00 (dd, 1H, $J_1 = 3.5$ Hz, $J_2 = 8.0$ Hz, C_4Et_4H), 1.42 (t, 3H, $J = 8.0$ Hz, CH_3CH_2CH), 1.41 (t, 3H, $J = 7.5$ Hz, CH_3), 1.11 (t, 3H, $J = 7.5$ Hz, CH_3), 0.99 (t, 3H, $J = 7.5$ Hz, CH_3). $^{13}C\{^1H\}$ NMR ($CDCl_3$): δ 294.8 (Mo=*C*Et), 139.1 (*C*Et), 116.6 (*C*Et), 102.6 (Cp), 76.5 (*C*HEt), 36.4 (CH_2), 24.4 (CH_2), 23.9 (CH_2), 20.3 (CH_2), 17.4 (CH_3), 14.5 (CH_3), 13.3 (CH_3), 9.2 (CH_3).

Crystal structure determinations

(a) Compound 4. Crystals for the X-ray structure analysis were grown from a slow diffusion of pentane in a CH_2Cl_2 solution at room temperature. A prism of $0.48 \times 0.36 \times 0.24$ mm^3 was cut from a red needle and sealed under argon in a capillary. A total of 25 reflections was used for an accurate orthorhombic cell determination and three reflections were selected to check the Laue group. A total of 1860 reflections were collected at room temperature up to $\sin(\theta)/\lambda = 0.623$ Å^{-1} on an Enraf-Nonius CAD4 diffractometer. The data were corrected for Lorentz and polarization effects[45] and for absorption (psi-scan method).[46] A 3% decay was linearly corrected. The structure was solved *via* a Patterson search program and refined in the polar space group $Pna2_1$ with full-matrix least squares methods[47] based on $|F^2|$. All non-hydrogen atoms were refined with anisotropic thermal parameters. Hydrogen atoms were included in their calculated positions and refined with a riding model. At the end of this refinement the agreement indices were $wR2 = 0.0526$ for all data and $R1 = 0.0196$ for 1764 intensities with $I > 2\sigma(I)$, the absolute structure parameter[48] was $x = 0.00(5)$ ($x = 0.19(5)$ and $wR2 = 0.0539$ for the inverted structure). The final difference electron density is featurless: $\Delta\rho = 0.256$ and -0.217 e Å^{-3}. Crystal data and final refinement parameters are reported in Table 5.

(b) Compound 5. A small red crystal of **5** ($0.05 \times 0.62 \times 0.12$ mm^3) suitable for an X-ray analysis was obtained by diffusion of pentane into a diethyl ether solution at 4 °C. The crystal was mounted on an Enraf-Nonius KappaCCD using Mo-Kα radiation and 10243 reflections (3924 unique) were collected up to $\sin(\theta)/\lambda = 0.65$ at 110 K. Absorption corrections were applied to the data during integration by the SCALEPACK algorithm.[49] The structure was solved *via* a Patterson search program and refined (space group $P\bar{1}$) with full-matrix least-squares methods based on $|F^2|$.[47] All non-hydrogen atoms were refined with anisotropic thermal parameters. Except for H(9), the hydrogen atoms of the complex were included in their calculated positions and refined with a riding model. The H(9) hydrogen atom attached to the C(9) carbon atom was located in a Fourier difference map and freely refined with an isotropic temperature factor. Final agreement indices are reported in Table 5.

CCDC reference number 186/1895.

See http://www.rsc.org/suppdata/dt/b0/b000948m/ for crystallographic files in .cif format.

Computational details

All calculations were performed using Gaussian 94[50] on an SGI Origin200 workstation. The LANL2DZ basis set was employed to perform geometry optimisations with a DFT approach. The three parameter form of the Becke, Lee, Tang and Parr functional (B3LYP)[51] was used in all cases. The LANL2DZ basis set includes both Dunning and Hay's D95 sets for H, C, N and O,[52]

Table 5 Crystal data and structure refinement for compounds **4** and **5**

Compound	**4**	**5**
Formula	$C_{19}H_{15}Cl_2Mo$	$C_{17}H_{26}Cl_2Mo$
M	410.15	397.22
T/K	293(2)	110(2)
Crystal system	Orthorhombic	Triclinic
Space group	$Pna2_1$	$P\bar{1}$
a/Å	18.958(6)	7.4272(4)
b/Å	12.485(1)	8.5344(3)
c/Å	7.187(1)	13.7739(6)
α/°		89.929(3)
β/°		79.954(3)
γ/°		86.459(2)
V/Å^3	1701.1(6)	858.01(7)
Z	4	2
λ/Å	0.71073	0.71073
Diffractometer	Nonius CAD4	Nonius Kappa CCD
μ/mm^{-1}	1.078	1.065
Crystal size/mm^3	0.48 × 0.36 × 0.24	0.050 × 0.062 × 0.118
RC = reflections collected	1860	10243
IRC = independent RC	1860	3924 [R(int) = 0.04]
IRCGT = IRC and [$I > 2\sigma(I)$]	1764	3546
R for IRCGT	$R1$ [a] = 0.0198, $wR2$ [b] = 0.0512	$R1$ [a] = 0.0312, $wR2$ [b] = 0.0673
R for IRC	$R1$ [a] = 0.0231, $wR2$ [b] = 0.0526	$R1$ [a] = 0.0378, $wR2$ [b] = 0.0716

[a] $R1 = \Sigma(|F_o| - |F_c|)/\Sigma|F_o|$. [b] $wR2 = [\Sigma w(F_o^2 - F_c^2)^2/\Sigma[w(F_o^2)^2]^{1/2}$ where $w = 1/[\sigma^2(F_o^2) + (0.0326P)^2 + 0.21P]$ for **4** and $w = 1/[\sigma^2(F_o^2) + 1.27P]$ for **5** and $P = (\mathrm{Max}(F_o^2, 0) + 2F_c^2)/3$.

and the relativistic Electron Core Potential (ECP) sets of Hay and Wadt for Mo and W.[53–55] The energies reported for the open shell (doublet) systems correspond to unrestricted B3LYP calculations. The mean value of the first-order wavefunction, which is not an exact eigenstate of S^2 for unrestricted calculations on the doublet systems, was considered suitable for the unambiguous identification of the spin state. Spin contamination was carefully monitored and the values of $\langle S^2 \rangle$ for the unrestricted B3LYP systems at convergence were very close to the ideal value of 0.75.

Acknowledgements

We are grateful to the MENRT, the CNRS and the Conseil Régional de Bourgogne for support of this work.

References

1 R. R. Schrock, *Science*, 1983, **219**, 13.
2 J. P. Collman, L. S. Hegedus, J. R. Norton and R. G. Finke, *Principles and Applications of Organotransition Metal Chemistry*, University Science Books, Mill Valley, CA, 1987.
3 W. E. Buhro and M. H. Chisholm, *Adv. Organomet. Chem.*, 1987, **27**, 311.
4 H. Yasuda and A. Nakamura, *Angew. Chem.*, *Int. Ed. Engl.*, 1987, **26**, 723.
5 A. Fürstner and G. Seidel, *Angew. Chem.*, *Int. Ed.*, 1998, **37**, 1734.
6 H. W. Gibson, in *Handbook of Conducting Polymers*, T. Skotheim, ed., Marcel Dekker, New York, 1986, vol. 1, p. 405.
7 H. H. Fox, M. O. Wolf, R. O'Dell, B. L. Lin, R. R. Schrock and M. S. Wrighton, *J. Am. Chem. Soc.*, 1994, **116**, 2827.
8 K. Weiss, A. Michel, E.-M. Auth, U. H. F. Bunz, T. Mangel and K. Müllen, *Angew. Chem.*, *Int. Ed. Engl.*, 1997, **36**, 506.
9 P. I. Dosa, C. Erben, V. S. Iyer, K. P. C. Vollhardt and I. M. Wasser, *J. Am. Chem. Soc.*, 1999, **121**, 10430.
10 M. Green, *Polyhedron*, 1986, **5**, 427.
11 J. L. Templeton, *Adv. Organomet. Chem.*, 1989, **29**, 1.
12 P. K. Baker, *Adv. Organomet. Chem.*, 1996, **40**, 45.
13 S. G. Bott, D. L. Clark, M. L. H. Green and P. Mountford, *J. Chem. Soc.*, *Dalton Trans.*, 1991, 471.
14 M. L. H. Green and P. Mountford, *Organometallics*, 1990, **9**, 886.
15 Q. Feng, M. L. H. Green and P. Mountford, *J. Chem. Soc.*, *Dalton Trans.*, 1992, 2171.
16 M. L. H. Green and P. Mountford, *Chem. Soc. Rev.*, 1992, 29.
17 P. Mountford, *J. Chem. Soc.*, *Dalton Trans.*, 1994, 1843.
18 M. L. H. Green, P. C. McGowan and P. Mountford, *J. Chem. Soc.*, *Dalton Trans.*, 1995, 1207.
19 A. J. Nielson, P. D. W. Boyd, G. R. Clark, P. A. Hunt, M. B. Hursthouse, J. B. Metson, C. E. F. Rickard and P. A. Schwerdtfeger, *J. Chem. Soc.*, *Dalton Trans.*, 1995, 1153.
20 I. M. Bartlett, S. Carlton, N. G. Connelly, D. J. Harding, O. D. Hayward, A. G. Orpen, C. D. Ray and P. H. Rieger, *Chem. Commun.*, 1999, 2403.
21 P. M. Boorman, M. Wang and M. Parvez, *J. Chem. Soc.*, *Dalton Trans.*, 1996, 4533.
22 Y.-C. Tsai, M. J. A. Johnson, D. J. Mindiola and C. C. Cummins, *J. Am. Chem. Soc.*, 1999, **121**, 10426.
23 S. F. Pedersen, R. R. Schrock, M. R. Churchill and H. J. Wasserman, *J. Am. Chem. Soc.*, 1982, **104**, 6808.
24 M. R. Churchill and H. J. Wasserman, *Organometallics*, 1983, **2**, 755.
25 M. B. O'Regan, M. G. Vale, J. F. Payack and R. R. Schrock, *Inorg. Chem.*, 1992, **31**, 1112.
26 J. L. Davidson, M. Green and F. G. A. Stone, *J. Chem. Soc.*, *Dalton Trans.*, 1977, 287.
27 J. L. Davidson, K. Davidson and W. E. Lindsell, *J. Chem. Soc.*, *Chem. Commun.*, 1983, 452.
28 J. L. Davidson, K. Davidson, W. E. Lindsell, N. W. Murrall and A. J. Welch, *J. Chem. Soc.*, *Dalton Trans.*, 1986, 1677.
29 L.-S. Wang, J. C. Fettinger and R. Poli, *J. Am. Chem. Soc.*, 1997, **119**, 4453.
30 E. Le Grognec, R. Poli and L.-S. Wang, *Inorg. Chem. Commun.*, 1999, **2**, 95.
31 M. D. Curtis, J. Real, W. Hirpo and W. M. Butler, *Organometallics*, 1990, **9**, 66.
32 O. J. Curnow, W. Hirpo, W. M. Butler and M. D. Curtis, *Organometallics*, 1993, **12**, 4479.
33 R. Poli, *Synlett.*, 1999, 1019.
34 Footnote 26 in ref. 16.
35 R. Poli, *J. Coord. Chem. B*, 1993, **29**, 121.
36 G. Smith, R. R. Schrock, M. R. Churchill and W. J. Youngs, *Inorg. Chem.*, 1981, **20**, 387.
37 M. D. Curtis, J. Real and D. Kwon, *Organometallics*, 1989, **8**, 1644.
38 M. D. Curtis and J. Real, *Organometallics*, 1985, **4**, 940.
39 D. Morales, R. Poli, P. Richard, J. Andrieu and E. Collange, *J. Chem. Soc.*, *Dalton Trans.*, 1999, 867.
40 J.-M. Camus, D. Morales, J. Andrieu, R. Poli, P. Richard, P. Braunstein and F. Naud, to be submitted.
41 A. Fries, M. Green, M. F. Mahon, T. D. MgGrath, C. B. M. Nation, A. P. Walker and C. M. Woolhouse, *J. Chem. Soc.*, *Dalton Trans.*, 1996, 4517.
42 J. R. Morrow, T. L. Tonker and J. L. Templeton, *J. Am. Chem. Soc.*, 1985, **107**, 5004.
43 R. G. Linck, B. E. Owens, R. Poli and A. L. Rheingold, *Gazz. Chim. Ital.*, 1991, **121**, 163.
44 R. Poli, in *Synthetic Methods of Organometallic and Inorganic Chemistry*, W. A. Herrmann, ed., Georg Thieme Verlag, Stuttgart, 1997, vol. 8, p. 101.

45 K. Harms, XCAD4, University of Marburg, 1996.
46 A. C. T. North, D. C. Phillips and F. S. Mathews, *Acta Crystallogr.*, *Sect. A*, 1968, **24**, 351. Implementation in PLATON: A. L. Spek, *Acta Crystallogr.*, *Sect. A*, 1990, **46**, C34.
47 G. M. Sheldrick, SHELXS and SHELXL97, University of Göttingen, Göttingen, Germany, 1997.
48 H. D. Flack, *Acta Crystallogr.*, *Sect. A*, 1983, **39**, 876.
49 Z. Otwinowski and W. Minor, *Methods Enzymol.*, 1997, **276**, 307.
50 M. J. Frisch, G. W. Trucks, H. B. Schlegel, P. M. W. Gill, B. G. Johnson, M. A. Robb, J. R. Cheeseman, T. A. Keith, G. A. Petersson, J. A. Montgomery, K. Raghavachari, M. A. Al-Laham, V. G. Zakrzewski, J. V. Ortiz, J. B. Foresman, J. Cioslowski, B. B. Stefanov, A. Nanayakkara, M. Challacombe, C. Y. Peng, P. Y. Ayala, W. Chen, M. W. Wong, J. L. Andres, E. S. Replogle, R. Gomperts, R. L. Martin, D. J. Fox, J. S. Binkley, D. J. Defrees, J. Baker, J. P. Stewart, M. Head-Gordon, C. Gonzales and J. A. Pople, Gaussian 94 (Revision E.1), Gaussian Inc., Pittsburgh, PA, 1995.
51 A. D. Becke, *J. Chem. Phys.*, 1993, **98**, 5648.
52 T. H. Dunning, Jr. and P. J. Hay, in *Modern Theoretical Chemistry*, H. F. Schaefer, III, ed., Plenum Press, New York, 1976, p. 1.
53 P. J. Hay and W. R. Wadt, *J. Chem. Phys.*, 1985, **82**, 270.
54 W. R. Wadt and P. J. Hay, *J. Chem. Phys.*, 1985, **82**, 284.
55 P. J. Hay and W. R. Wadt, *J. Chem. Phys.*, 1985, **82**, 299.
56 E. Le Grognec, R. Poli and P. Richard, to be submitted.
57 C. K. Johnson, ORTEP, Report ORNL-5138, Oak Ridge National Laboratory, Oak Ridge, TN, 1976.